Manganese dioxide modified silicon nanowires and their excellent catalysis in the decomposition of methylene blue

Weiwei Gao, Mingwang Shao, Li Yang, Shujuan Zhuo, Shiyong Ye, and Shuit-tong Lee

Citation: Applied Physics Letters **100**, 063104 (2012); doi: 10.1063/1.3682486
View online: http://dx.doi.org/10.1063/1.3682486
View Table of Contents: http://scitation.aip.org/content/aip/journal/apl/100/6?ver=pdfcov
Published by the AIP Publishing

Manganese dioxide modified silicon nanowires and their excellent catalysis in the decomposition of methylene blue

Weiwei Gao,[1,2] Mingwang Shao,[1,a)] Li Yang,[1,2] Shujuan Zhuo,[1] Shiyong Ye,[2,a)] and Shuit-tong Lee[3]

[1]*Jiangsu Key Laboratory for Carbon-Based Functional Materials and Devices, Institute of Functional Nano and Soft Materials Laboratory (FUNSOM), Soochow University, Suzhou, Jiangsu 215123, People's Republic of China*

[2]*Anhui Key Laboratory of Functional Molecular Solids, College of Chemistry and Materials Science, Anhui Normal University, Wuhu 241000, People's Republic of China*

[3]*Center of Super-Diamond and Advanced Films (COSDAF) and Department of Physics and Materials Science, City University of Hong Kong, Hong Kong SAR, China*

(Received 4 December 2011; accepted 17 January 2012; published online 6 February 2012)

A redox between hydrofluoric acid and ammonium fluoride-treated silicon nanowires and potassium permanganate solution was investigated. The results showed that MnO_2 nanoparticles might grow on the surface of silicon nanowires, which was confirmed with the transmission electron microscope. These MnO_2 modified silicon nanowires were employed as catalysts in the decomposition of methylene blue using sodium borohydride as the reducing agent, which exhibited excellent catalysis with its reaction rate 6 times larger than the unsupported MnO_2. [doi:10.1063/1.3682486]

Silicon nanowires (SiNWs) have various potential applications.[1–3] Being one of the most prevalent semiconductors, they have many unique properties, such as large surface-to-volume ratio,[4] stability to atmospheric environment,[5] and ease of modification.[6]

Currently, one obvious challenge is to utilize these 1D silicon nanostructures as silicon mats to anchor metal oxide materials with potential application in different fields.

Manganese oxides have attracted considerable research interest due to their distinctive physical and chemical properties and wide applications in catalysis,[7] magnetic storage,[8] ion exchange,[9] electrode materials,[10–12] and sensors.[13] Among them, manganese dioxide (MnO_2) has been considered as the promising one for its excellent catalytic activity.

For the above advantages of SiNWs and manganese dioxide, we developed simple strategy to synthesize MnO_2/SiNWs. The entire reactions proceeded at room temperature within 3 min without adding any organic auxiliary agent. The obtained MnO_2/SiNWs were employed as catalysts in the decomposition of methylene blue (MB) using sodium borohydride (SB) as a reducing agent. Compared to other report,[14] MnO_2/SiNWs showed exhibited high catalytic activity in the decomposition of methylene blue.

Potassium permanganate ($KMnO_4$) and manganese (II) chloride tetrahydrate ($MnCl_2{\cdot}4H_2O$) supplied from National Pharmaceutical Group Chemical Reagent Co. Ltd. were used directly without any further purification. SB and MB were purchased from Alfa Aesar. Other chemicals used were of analytical grade, and the corresponding solutions were prepared using double-distilled water.

The phase purity of the as-prepared products was determined by a Shimadzu XRD-6000 x-ray diffractometer equipped with Cu Kα radiation ($\lambda = 0.15406$ nm). A scanning rate of 0.05° s^{-1} was applied to record the pattern. Transmission electron microscope (TEM) was captured with a FEI Tecnai F20 transmission electron microscope, with an accelerating voltage of 200 kV. X-ray photoelectron spectroscopy (XPS) was recorded on a VGESCALAB MK II x-ray photoelectron spectrometer, using non-monochromatized Al Kα x-ray as the excitation source. UV-vis absorption spectra were obtained using a PerkinElmer Lambda 750 spectrophotometer at room temperature under ambient conditions. Inductively coupled plasma-atomic emission spectrometry (ICP-AES) was taken with ICP-AES analyzer (Vista MPX).

SiNWs (0.01 g) were obtained by using the oxide-assisted growth method,[15] and then etched with 10 mL 5% HF aqueous solution for 10 s to remove their outer oxide layer to become hydrogen-terminated SiNWs (H-SiNWs). The H-SiNWs were rinsed with distilled water and immersed in 15 mL 0.1 M $KMnO_4$ aqueous solution. When the color of the SiNWs changed from yellow to gray black, it meant that $KMnO_4$ was reduced to MnO_2 by the H-SiNWs and the MnO_2/SiNWs were obtained. The fabrication of MnO_2/SiNWs was illustrated in Fig. 1.

The preparation of unsupported MnO_2 nanoparticles with average diameter of 25 nm was based on the redox reaction between $MnCl_2{\cdot}4H_2O$ and $KMnO_4$. $KMnO_4$ (0.25 mL, 0.2 M) and $MnCl_2{\cdot}4H_2O$ (0.25 mL 0.3 M) were added into 50 mL water, which was sonicated for 1 h to obtain the unsupported MnO_2 nanoparticles. This process may be expressed as $2MnO_4^- + 3Mn^{2+} + 2H_2O = 5MnO_2 + 4H^+$.

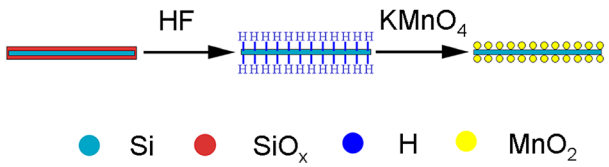

FIG. 1. (Color online) Schematic for the fabrication of MnO_2/SiNWs.

a)Authors to whom correspondence should be addressed. Electronic mail: mwshao@mail.ahnu.edu.cn and ahnuysy@yahoo.com.cn.

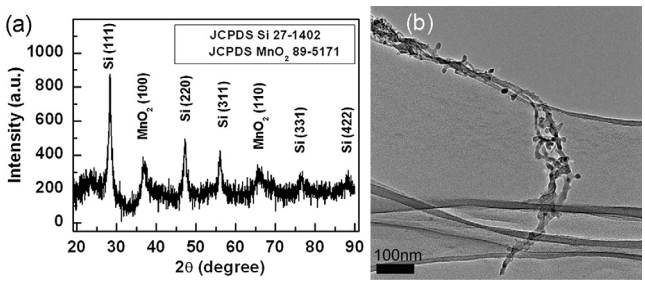

FIG. 2. (a) XRD pattern of the MnO_2/SiNWs; (b) TEM image of MnO_2/SiNWs.

In a typical catalytic process, SB was dissolved with ice-cold distilled water and preserved in an ice-water bath. At the same time, 100 μl (1×10^{-3} M) of MB solution was mixed with defined amount double-distilled water and purged with N_2 gas for 5–6 min to remove all dissolved oxygen. Then, the as-prepared MnO_2/SiNWs (0.001 g, the amount of containing MnO_2 is 5.5×10^{-4} g determined with ICP-AES) catalysts and 1×10^{-2} M (50, 75, 100, 125, or 150 μl) of freshly prepared SB were added. The progress of the reaction was monitored using a UV-vis spectrophotometer.

The phases of the prepared MnO_2/SiNWs were investigated by the XRD analysis as shown in Fig. 2(a), which displayed no other characteristic peaks except MnO_2 and Si. The peaks at 2θ around 28, 47, 56, 76, and 88° correspond to the (111), (220), (311), (331), and (422) diffraction peaks of Si. And, the calculated cell parameter is $a = 0.54296 \pm 0.0006$ nm, which matches the value of face-centered cubic silicon $a = 0.5430$ nm (JCPDS card No. 27-1402). The diffraction peaks at 36° and 65° may be indexed as (100) and (110) diffraction planes of hexagonal MnO_2, respectively (JCPDS card No. 30-0820).

The TEM image in Fig. 2(b) shows the morphologies of MnO_2/SiNWs. When $KMnO_4$ was reacted with H-SiNW for 3 min, the deposited MnO_2 particles are spherical with the average diameter of 10 nm as shown in Fig. 2(b). After $KMnO_4$ was reacted with H-SiNW for 5 min, we found that the formation of MnO_2 nanoflowers with average diameter of 150 nm wrapped on surface of SiNWs.

This phenomenon was resulted from the reaction between $KMnO_4$ and H-SiNWs, according to following reaction:

$$KMnO_4 + \text{H-SiNWs} \rightarrow MnO_2/\text{SiNWs}. \quad (1)$$

Yet, if the reaction time was too long, the produced MnO_2 nanoparticles will grow up to become very big nanoflowers.

To analyze the elemental composition as well as the chemical-bonding environment of MnO_2/SiNWs, XPS measurement was conducted on MnO_2/SiNWs (Fig. 3). Figure 3(a) shows the full spectrum of MnO_2/SiNWs using C1s as reference at 284.6 eV. No peaks of other elements except C, O, Si, and Mn are observed. The core spectra in the Mn2p region of MnO_2/SiNWs show the presence of $Mn2p_{3/2}$ and $Mn2p_{1/2}$ peaks at 642.2 and 653.9 eV (Fig. 3(b)), which may be attributed to MnO_2 as the previous reports.[16]

To investigate MnO_2/SiNWs' catalysis, they were employed as catalysts in the reduction of MB in the presence of SB. The UV-vis spectrophotometer was employed to monitor the decomposition of methylene blue (Fig. 4). Figure 4(a) reveals that there exist linear relations between the logarithm of C_{MB} and time under different volume of SB. Simultaneously, it can be observed that the reaction takes place very fast using MnO_2/SiNWs as catalysts, and the reduction rate increased with the amount of SB increased. It is apparent that the reduction is a first-order reaction to the concentration of MB. The reduction rate of MB may be usually expressed as $r = kC_{SB}^{m}C_{MB}^{n}$ mol/min. When the reaction order to concentration of MB is confirmed, the reaction order to concentration of SB may be calculated in Fig. 4(b). Figure 4(b) shows the relationship of reaction rate vs C_{SB}, which is proportional to the square root of C_{SB} obtained from the slope of Fig. 4(b). The linear relationship may be expressed as $\text{LogK} = 4.59964 + 0.99417\ \text{Log}C_{SB}$. The reduction is also a first-order reaction to the concentration of SB judged from this equation. By combining with Figs. 4(a) and 4(b), the reduction rate of MB can be expressed as $r = 111.5\ C_{SB}\ C_{MB}$ mol/min.

Figure 4(c) shows UV-vis spectra of the reduction by MnO_2/SiNW catalysts under the SB concentration of 5×10^{-4} M, which reveals that the reduction takes place fast. In order to have a comparison, a series of UV-vis spectra were collected using 0.001 g unsupported MnO_2 catalysts (Fig. 4(d)) in the same reduction system. Overall, it demonstrates high and excellent catalysis of MnO_2/SiNWs. In order to further highlight the outstanding catalytic activity of MnO_2/SiNWs, the linear relations between the logarithm of C_{MB} and time were accomplished in different catalyst condition. And error bar was made for three repeated trials of each time point using MnO_2/SiNW catalysts (Fig. 5). The reaction rate of MnO_2/SiNW catalysts is 6 times larger than that of MnO_2, and 60 times that of SiNWs or no catalysts obtained from Fig. 5. The above results obviously indicate that the

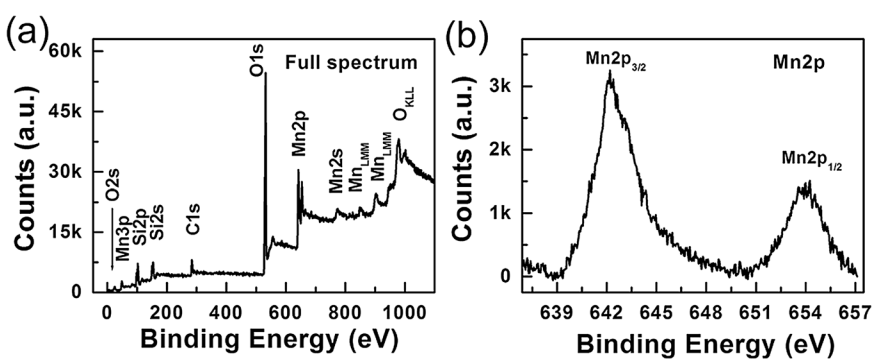

FIG. 3. (a) Wide scan XPS full spectrum of MnO_2/SiNWs; (b) core spectrum of Mn2p.

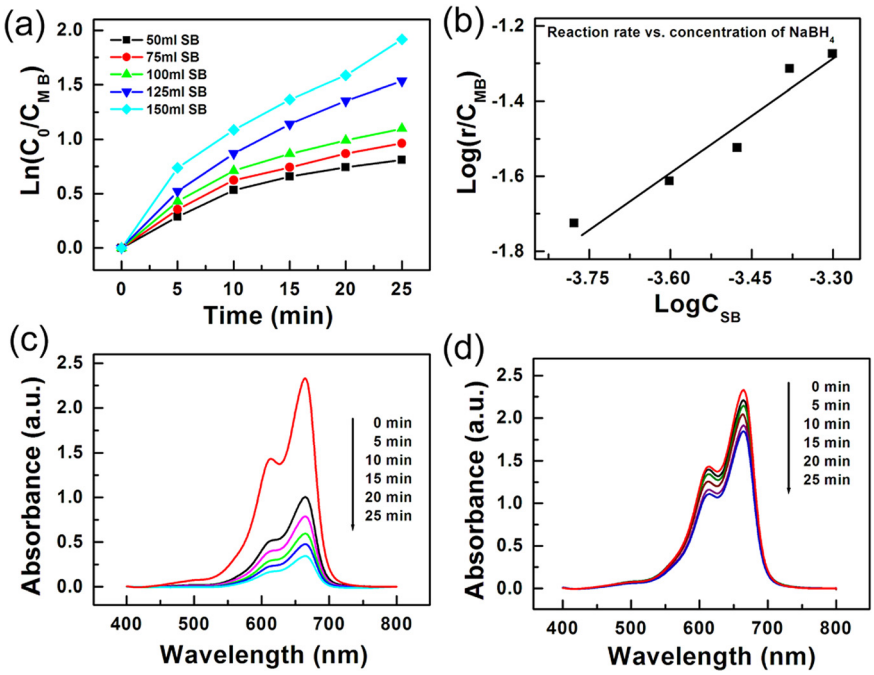

FIG. 4. (Color online) (a) Curves of concentration vs time at various amount of SB (1×10^{-2} M); (b) curve of reaction rate vs concentration of SB; and UV-vis spectra of the reduction under the SB concentration of 3×10^{-4} M by (c) MnO_2/SiNWs and (d) unsupported MnO_2.

excellent catalytic activity of MnO_2/SiNW catalysts. The significant catalysis of MnO_2/SiNW catalysts is promising, which may find wide applications in the catalytic field.

With regard to the catalytic mechanism of the reduction, the MnO_2 nanoparticles with an intermediate redox potential value of the donor-acceptor partner plays an important role during the electron-transfer step and acts as an electron transfer system. In our experiment, MnO_2 nanoparticles with an average diameter of 10 nm have a large surface-to-volume ratio. It is possible to adsorb a great quantity of MB onto the nanoparticle surface, which may bring high activity to the as-prepared catalysts. Whereas SiNWs act as a carrier to support MnO_2 nanoparticles, the nanoparticles are kept from congregating because they are fixed by the SiNWs, which makes it possible for them to have high catalytic efficiency. Although unsupported MnO_2 nanoparticles also revealed this size effect, their size might gradually grow large during the process of reaction and thus decreased the catalysis activity.

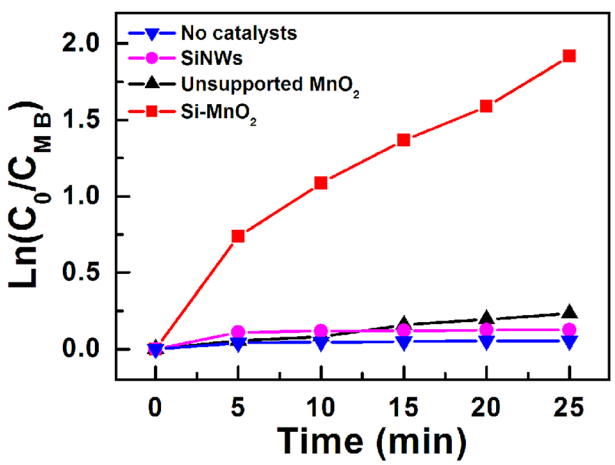

FIG. 5. (Color online) Curves of MB concentration vs time using MnO_2/SiNW catalysts, unsupported MnO_2, SiNWs, and no catalysts under the SB concentration of 5×10^{-4} M.

MnO_2/SiNWs was prepared by solution approach. Compared to other methods, solution method is simple, fast and cost effective. At the same time, the MnO_2/SiNWs were employed as catalysts in the decomposition of methylene blue using sodium borohydride as the reducing agent. The results indicated that MnO_2/SiNWs possessed the excellent catalytic activity, which might find potential application in the catalytic field.

The project was supported by the National Natural Science Foundation of China (21071106), Specialized Research Fund for the Doctoral Program of Higher Education (20103201110016), and the National Basic Research Program of China (973 Program) (Grant No. 2012CB932903).

[1]C. S. Guo, L. B. Luo, G. D. Yuan, X. B. Yang, R. Q. Zhang, W. J. Zhang, and S. T. Lee, Angew. Chem. Int. Ed. **48**, 9896 (2009).
[2]Y. Q. Qu, H. L. Zhou, and X. F. Duan, Nanoscale **3**, 4060 (2011).
[3]F. Y. Wang, Q. D. Yang, G. Xu, N. Y. Lei, Y. K. Tsang, N. B. Wong, and J. C. Ho, Nanoscale **3**, 3269 (2011).
[4]V. Schmidt, J. V. Wittemann, S. Senz, and U. Gosele, Adv. Mater. **21**, 2681 (2009).
[5]G. D. Yuan, Y. B. Zhou, C. S. Guo, W. J. Zhang, Y. B. Tang, Y. Q. Li, Z. H. Chen, Z. B. He, X. J. Zhang, P. F. Wang, I. Bello, R. Q. Zhang, C. S. Lee, and S. T. Lee, ACS Nano **4**, 3045 (2010).
[6]M. W. Shao, D. D. D. Ma, and S. T. Lee, Eur. J. Inorg. Chem. **27**, 4264 (2010).
[7]S. Ching, D. A. Kriz, K. M. Luthy, E. C. Njagi, and S. L. Suib, Chem. Commun. **47**, 8286 (2011).
[8]T. D. Schladt, T. Graf, and W. Tremel, Chem. Mater, **21**, 3183 (2009).
[9]Z. H. Liu, L. P. Kang, M. Z. Zhao, and K. Ooi, J. Mater. Res. **22**, 2437 (2007).
[10]Q. Li, K. X. Li, J. Y. Gu, and H. Fan, J. Phys. Chem. Solid **69**, 1733 (2008).
[11]S. J. Ling, R. Yuan, Y. Q. Chai, and T. T. Zhang, Bioproc. Biosyst. Eng. **32**, 407 (2009).
[12]D. Y. Sung, I. Y. Kim, T. W. Kim, M. S. Song, and S. J. Hwang, J. Phys. Chem. C **115**, 13171 (2011).
[13]C. N. Xu, K. Miyazaki, and T. Watanabe, Sens. Actuat. B **46**, 87 (1998).
[14]T. Sriskandakumar, N. Opembe, C. H. Chen, A. Morey, C. King'ondu, and S. L. Suib, J. Phys. Chem. A **113**, 1523 (2009).
[15]M. W. Shao, Y. Y. Shan, N. B. Wong, and S. T. Lee, Adv. Funct. Mater. **15**, 1478 (2005).
[16]J. Chastain, *Handbook of X-ray Photoelectron Spectroscopy* (Perkin-Elmer Corporation, Eden Prairie, MN, 1992).